

RESEARCH ARTICLE

# A New Role of the Mosquito Complement-like Cascade in Male Fertility in *Anopheles gambiae*

Julien Pompon<sup>1\*</sup>, Elena A. Levashina<sup>1,2\*</sup>

**1** CNRS UPR9022, Inserm U963, Université de Strasbourg, Institut de Biologie Moléculaire et Cellulaire, Strasbourg, France, **2** Max Planck Institute for Infection Biology, Berlin, Germany

✉ Current address: Programme in Emerging Infectious Diseases, Duke-NUS Graduate Medical School, Singapore

\* [levashina@mpiib-berlin.mpg.de](mailto:levashina@mpiib-berlin.mpg.de)



CrossMark  
click for updates

 OPEN ACCESS

**Citation:** Pompon J, Levashina EA (2015) A New Role of the Mosquito Complement-like Cascade in Male Fertility in *Anopheles gambiae*. PLoS Biol 13(9): e1002255. doi:10.1371/journal.pbio.1002255

**Academic Editor:** David S. Schneider, Stanford University, UNITED STATES

**Received:** March 19, 2015

**Accepted:** August 14, 2015

**Published:** September 22, 2015

**Copyright:** © 2015 Pompon, Levashina. This is an open access article distributed under the terms of the [Creative Commons Attribution License](http://creativecommons.org/licenses/by/4.0/), which permits unrestricted use, distribution, and reproduction in any medium, provided the original author and source are credited.

**Data Availability Statement:** All relevant data are within the paper and its Supporting Information files.

**Funding:** This work was supported by funds from the European Union's Seventh Framework Program (FP7/2007-2013 [http://ec.europa.eu/research/health/ongoing-fp7\\_en.html](http://ec.europa.eu/research/health/ongoing-fp7_en.html)) under grant agreements N° 242095 (EVI-Malar) and N° 223601 (MALVECBLOK), by the ANR (<http://www.agence-nationale-recherche.fr>) grant GIME (ANR-11-BSV7-009-01). JP was supported by fellowships from FRM and the Fondation les Treilles. The funders had no role in study design, data collection and analysis, decision to publish, or preparation of the manuscript.

## Abstract

Thioester-containing protein 1 (TEP1) is a key immune factor that determines mosquito resistance to a wide range of pathogens, including malaria parasites. Here we report a new allele-specific function of TEP1 in male fertility. We demonstrate that during spermatogenesis TEP1 binds to and removes damaged cells through the same complement-like cascade that kills malaria parasites in the mosquito midgut. Further, higher fertility rates are mediated by an allele that renders the mosquito susceptible to *Plasmodium*. By elucidating the molecular and genetic mechanisms underlying TEP1 function in spermatogenesis, our study suggests that pleiotropic antagonism between reproduction and immunity may shape resistance of mosquito populations to malaria parasites.

## Author Summary

While Anopheline mosquitoes are the most efficient vectors of human malaria, they do have protective mechanisms directed against the causative parasite, *Plasmodium falciparum*. Their immune system targets the invading parasites through activation of the mosquito complement-like system. A central component of this system, thioester-containing protein 1 (TEP1), is a highly polymorphic gene with four allelic classes. Although one class, called R1, mediates efficient parasite elimination, the other classes render the mosquitoes susceptible to *Plasmodium* infections. Until now, it was not clear how or why any of these susceptible *TEP1* alleles were maintained in the population. Here we discover a new role of TEP1 in male fertility. We demonstrate that mosquitoes use the same mechanism—nitration of target surfaces—to flag both damaged sperm and *Plasmodium* cells. Binding of TEP1 to, and removal of, the aberrant sperm is critical to preserve high fertility rates. In the absence of TEP1, accumulation of damaged sperm degrades male fertility. Surprisingly, in spite of the common mechanism of TEP1 activation, distinct alleles of *TEP1* mediate efficient removal of defective sperm and killing of malaria parasites. Our

**Competing Interests:** The authors have declared that no competing interests exist.

**Abbreviations:** ANOVA, analysis of variance; APL1C, *Anopheles Plasmodium*-responsive leucine-rich protein 1C; dsRNA, double-stranded RNA; GFP, green fluorescent protein; GSC, germline stem cell; Gy, gray; HPX2, heme peroxidase 2; HPX15, heme peroxidase 15; LRIM1, leucine-rich immune protein 1; MAG, male accessory gland; NOX5, NADPH oxidase 5; PPO2, prophenoloxidase 2; qRT-PCR, quantitative reverse transcription PCR; RFLP, restriction fragment length polymorphism; RNS, reactive nitrogen species; RPL19, ribosomal protein L19; SE, standard error; SEM, standard error of the mean; SSC, somatic stem cell; TEP1, thioester-containing protein 1; TUNEL, TdT-mediated dUTP nick-end labeling.

results suggest that pleiotropic function in immunity and reproduction is one of the mechanisms that maintain *TEP1* polymorphism in mosquito populations.

## Introduction

*Anopheles gambiae* mosquitoes are the most efficient vectors of human malaria. Mosquitoes actively respond to *Plasmodium* infections by mounting immune responses that destroy the majority of invading parasites. These responses are largely mediated by thioester-containing protein 1 (TEP1) [1–4], a homologue of the mammalian complement factor C3. TEP1 is synthesized in the mosquito blood cells and is secreted into the blood or hemolymph, where a protein cascade called “mosquito complement-like system” tightly controls its activity. A series of studies on TEP1-mediated killing of *Plasmodium* parasites demonstrated that a complex of two leucine-rich repeat proteins, leucine-rich immune protein 1 (LRIM1) and *Anopheles Plasmodium*-responsive leucine-rich protein 1C (APL1C), prevents precocious activation of TEP1 [5,6], whereas heme peroxidase 2 (HPX2) and NADPH oxidase 5 (NOX5) oxidases direct TEP1 binding to *Plasmodium* by modifying ookinete surfaces [7]. Elimination of any of these factors does not affect *TEP1* expression but abolishes its binding to parasites and increases mosquito susceptibility to infections [2,7–9]. However, TEP1 function was only examined in the immune responses of females, which are responsible for malaria transmission.

Here we report a new function of TEP1 in male fertility. We demonstrate that TEP1 and other members of the complement-like cascade are present in the testes and uncover an allele-specific *TEP1* contribution to clearance of apoptotic cells during spermatogenesis. We also show that TEP1 binding to defective sperm cells is regulated by the same complement-like cascade that kills malaria parasites in the mosquito midgut. In spite of these similarities, our results demonstrate that male fertility is promoted by the *TEP1*\*S2 allele, which renders mosquitoes susceptible to *Plasmodium* infections. By elucidating the molecular and genetic mechanisms underlying TEP1 function in reproduction, our study reveals an example of pleiotropic antagonism between alleles that may impact the genetic makeup of the mosquito resistance to *Plasmodium*.

## Results

### TEP1 Occurrence in the Mosquito Testis

Using polyclonal antibodies and confocal microscopy of dissected whole mount testes, we observed TEP1 signal in the spermatogenic compartments of *A. gambiae*. The mosquito spermatogenic compartments are distinguished by the shape of the sperm nuclei [10] and by the expression pattern of  $\beta$ -tubulin [11]. The apical side of the testes contains a ring of hub cells, the niche of the germline stem cells (GSC) and somatic stem cells (SSC). Upon division, GSCs differentiate into the primary spermatogonia. These compartments do not express the  $\beta$ -tubulin gene whose expression begins in the spermatocytes. All sperm cells from the hub to the spermatocytes display rounded nuclei, whereas the nuclei of the spermatids and spermatozoa adopt their mature elongated shape. To facilitate mapping of TEP1-positive cells in the testes, we made use of the *DSX* transgenic line in which  $\beta$ -tubulin gene promoter directed the expression of green fluorescent protein (GFP) reporter in spermatocytes, spermatids, and spermatozoa (Fig 1A and 1B) [12]. TEP1 signal was detected on spermatogonia (round nuclei, no expression of  $\beta$ -tubulin::eGFP, Fig 1C) and on spermatozoa (elongated nuclei, expression of  $\beta$ -tubulin::eGFP, Fig 1D and 1E). Given this surprising localization, we tested whether TEP1

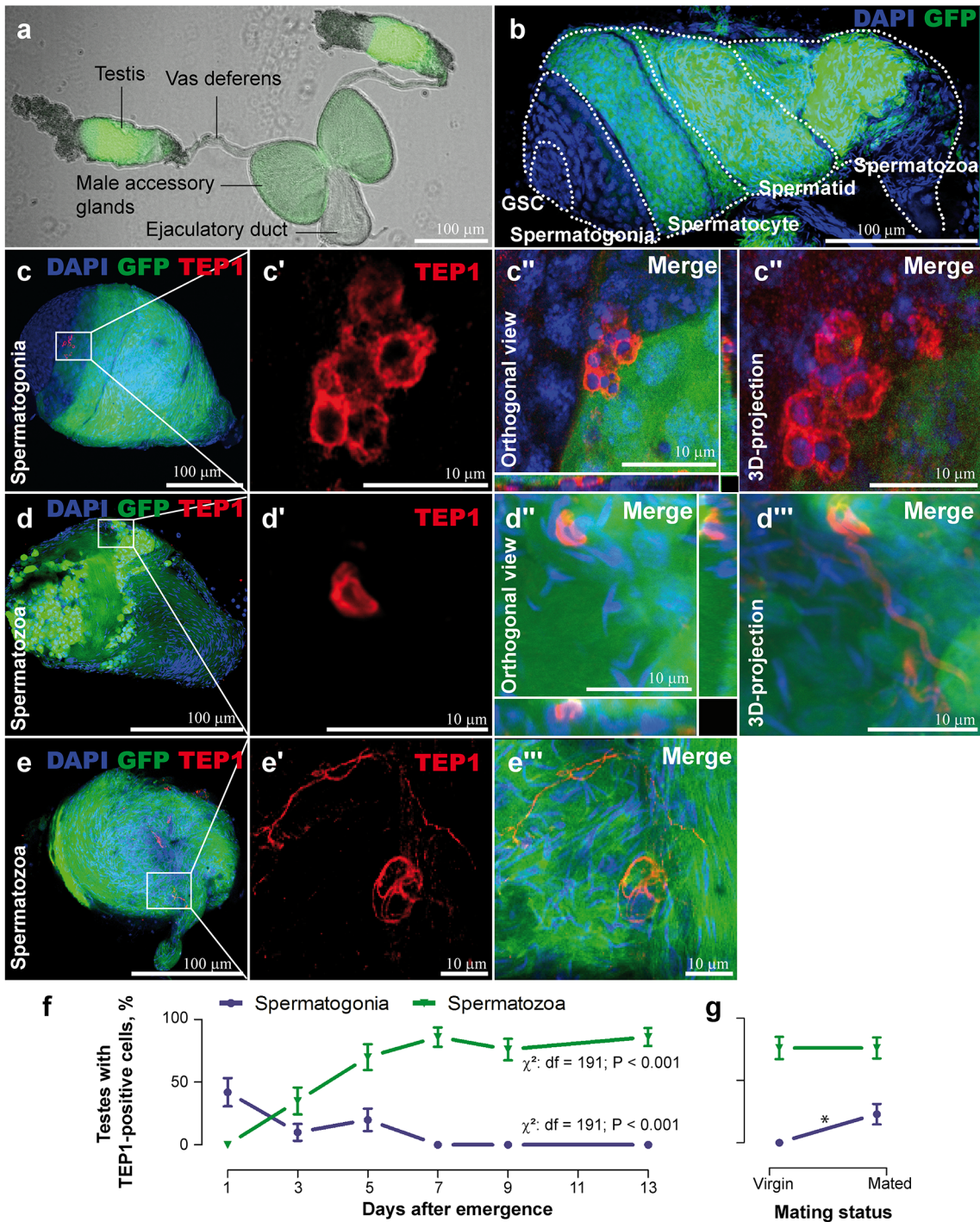


**Fig 1. TEP1 occurrence in the testes during spermatogonial development.** The *DSX* transgenic line [12] that expresses *GFP* (green) under the  $\beta$ -*tubulin* promoter in the meiotic stages starting from spermatocytes but not in the mitotic germline stem cells (GSC) and spermatogonia. Nuclei were colored with DAPI (blue). (A) Male reproductive organs. (B) Organization of spermatogonial compartments in the testis (dotted lines). (C–E) TEP1 (red) recruitment to the spermatogonia (C–C'') and to the spermatozoa's head (D–D'') and tail (E–E''). (F) Occurrence of testes with TEP1-positive cells during the first week after adult emergence. Testes were dissected for immunofluorescence analyses at the indicated time points. (G) Effect of mating on the percentage of testes with TEP1-positive cells. Virgin males (7-d-old) were collected in copula, and 2 d later their testes were dissected for immunofluorescence analyses. Significant differences ( $p < 0.05$ ,  $\chi^2$  test) are shown by an asterisk. Vertical bars show standard deviation,  $n \geq 30$  testes. Data used to make this figure can be found in [S1 Data](#).

doi:10.1371/journal.pbio.1002255.g001



expression correlates with spermatogonial development, which in mosquitoes is initiated at the larval stages and is completed a couple of days after the emergence of adults [10,13]. In *Anopheles* males, copulation triggers a new wave of spermatogenesis to replenish the ejaculated spermatozoa [10]. Therefore, we monitored the occurrence of TEP1 signal in the testes of virgin males during the first 2 wk after adult emergence and after mating. The percentage of testes with TEP1-positive spermatogonia decreased during the first week after male emergence and correlated with the termination of spermatogenesis (Fig 1F). Consistent with the onset of sperm production, the proportion of testes with TEP1-positive spermatogonia increased after mating (Fig 1G). In contrast, spermatogenesis did not promote the occurrence of TEP1-positive spermatozoa, whose numbers were increasing with time after adult emergence. These data suggest that TEP1 occurrence in the testes correlates with spermatogenic development.

## The Conserved Complement-like Cascade Directs TEP1 Binding to Damaged Sperm for Removal

As spermatogenesis is accompanied by waves of apoptosis [14,15], we asked whether TEP1 was recruited to defective spermatogonia. To this end, massive sperm damage was experimentally induced in *DSX* pupae by radiation [10,16]. We first gauged the impact of radiation on male fertility and confirmed that it drastically decreased hatching rates of the progeny (Fig 2A and 2B). A significant reduction in egg laying was only observed in females mated with the *DSX* males irradiated with the highest dose (100 Gray [Gy]). Further, we observed a significant increase in the proportion of testes with TEP1-positive spermatogonia, which correlated with the reduction in the size of the spermatogonial compartment in 3-d-old irradiated *DSX* males (Fig 2C–2E, S1 Fig), suggestive of TEP1 recruitment to defective cells. Indeed, radiation significantly increased the number of damaged cells, as measured by TdT-mediated dUTP nick-end labeling (TUNEL), which marks DNA breaks associated with cell death. Interestingly, all TEP1-positive cells in the testes of control and irradiated males were TUNEL positive, but not all TUNEL-positive cells were also stained with the anti-TEP1 antibody (Fig 2F). Moreover, radiation-induced cell damage and TEP1 signal were also detected in the GFP-negative germline compartment (Fig 2G). These results suggest that TEP1 is recruited to damaged cells.

The specificity of the detected TEP1 signal was confirmed by two independent approaches. First, we used a mosquito transgenic line (7b) in which *TEP1* expression is constitutively repressed by a dominant transgene-mediated silencing (S2 Fig). Second, we injected irradiated *DSX* males with double-stranded RNA (dsRNA) against *TEP1* 1 d after emergence. TEP1 signal was not detected in the testes of irradiated males in both TEP1 depletion methods, confirming signal specificity (Fig 2H, S2 Fig). We next examined whether other members of the complement-like cascade were present in the testes, using polyclonal antibodies against LRIM1 and HPX2 and confocal microscopy. Neither LRIM1 nor HPX2 signals associated with the sperm cells, but they were detected in the cells attached to the testes (S3 Fig). Since elimination of any of these factors does not affect TEP1 expression but abolishes TEP1 binding to parasites [2,7–9], we exploited their silencing to discriminate whether TEP1 is expressed in or bound to the sperm cells. Depletion of either protein abolished TEP1 signal on spermatogonia but did not affect TEP1 expression, as evidenced by a clear TEP1 signal detected by immunoblotting in the hemolymph extracts of males (Fig 2H, S4 Fig), supporting the hypothesis that the observed signal resulted from TEP1 binding to spermatogonia. Taken together, these results demonstrate that the complement-like cascade regulates TEP1 binding to defective sperm.

In mammals, complement contributes to the removal of apoptotic cells [17]. Therefore, we examined whether TEP1 binding mediated clearance of defective spermatogonia by comparing the number of TUNEL-positive cells in the testes of control and TEP1-depleted males in a

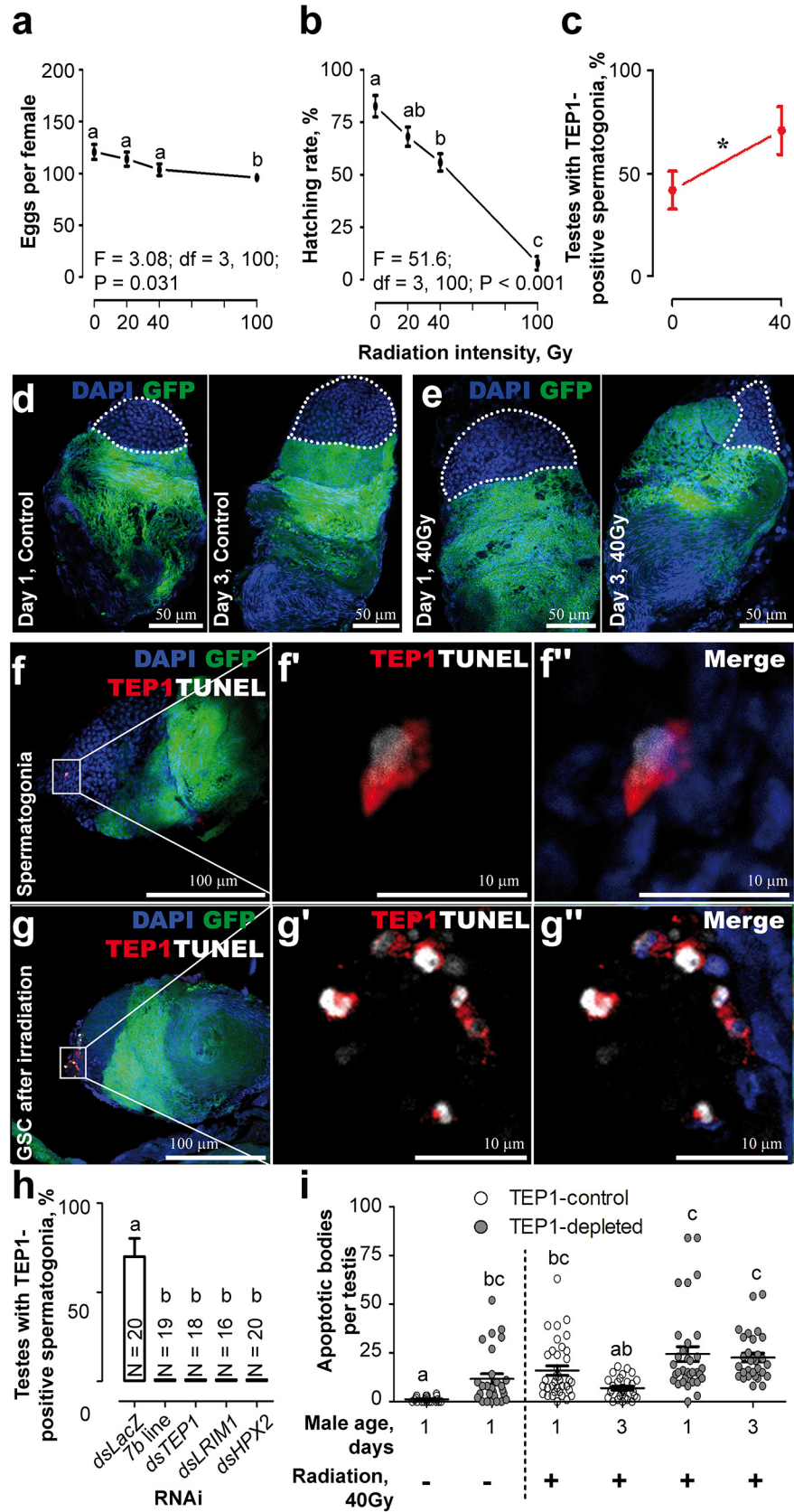


**Fig 2. Effect of radiation on TEP1-mediated removal of damaged sperm.** A *DSX* transgenic line expressing *GFP* (green) under the  $\beta$ -*tubulin* promoter was used. Nuclei were colored with DAPI (blue). (A,B) 3-d-old virgin males that emerged from irradiated pupae were mated with 3-d-old virgin females, and the number of (A) laid eggs and the (B) larval hatching rates per female were gauged. Means  $\pm$  standard error of the mean (SEM) are plotted for  $n \geq 25$ . (C) The proportion of testes with TEP1-positive spermatogonia in irradiated males (40 Gy),  $n \geq 30$ . (D,E) Radiation (40 Gy) reduces the size of the spermatogonial compartment (white dotted line) in 1- and 3-d-old males. (F,G) Colocalization of TEP1 (red) and TUNEL (white) signals in (F–F’’) spermatogonia and (G–G’’) the GSC in irradiated 1-d-old males. (H) Occurrence of TEP1 in spermatogonia of irradiated (40 Gy) males (*DSX*) injected with *dsTEP1*, *dsLRIM1*, *dsHPX2*, and *dsLacZ* (control). Males depleted for *TEP1* (7*b* line) served as positive controls. The proportion of testes with TEP1 signal was gauged 2 d later. Mean  $\pm$  standard error (SE) is shown; N, number of testes. (i) Accumulation of TUNEL-positive spermatogonia after irradiation in the testes of control and TEP1-depleted males (progeny of reciprocal crosses between 7*b* and *DSX*) was examined 1 and 3 d after emergence. Each dot represents one testis. Significant differences ( $p < 0.05$ ,  $\chi^2$  test) are shown by an asterisk and by characters above the corresponding values. Data used to make this figure can be found in [S1 Data](#).

doi:10.1371/journal.pbio.1002255.g002

similar genetic background of the F<sub>1</sub> progeny of a reciprocal cross between *DSX* and 7*b* ([S5 Fig](#)). Significantly higher numbers of TUNEL-positive cells were detected in the absence of TEP1 in the testes of freshly emerged males ([Fig 2I](#), day 1). Furthermore, while irradiation increased the number of damaged cells in all samples, their numbers decreased with time in controls but remained high in TEP1-depleted mosquitoes ([Fig 2I](#), day 3). These results suggest that TEP1 binding to the spermatogonia correlates with removal of defective cells during spermatogenesis.

## TEP1 Rescues Radiation-Induced Male Infertility

Based on these results, we proposed that TEP1 marks damaged spermatogonia for removal. Accumulation of dead cells degrades sperm quality [18]. Therefore, we hypothesized that TEP1 deficiency should decrease male fertility after irradiation. Indeed, radiation significantly decreased larval hatching rates ([Fig 3A](#)). Importantly, a larger decrease was observed in the progeny of TEP1-depleted males as compared to controls, suggesting that TEP1 partially rescues radiation-induced male sterility.

*TEP1* is a highly polymorphic gene with four major alleles that differ in their capacity to kill or to resist malaria parasites—namely, the resistance-associated alleles *R1* and *R2* and the susceptibility-associated alleles *S1* and *S2* [19–22]. Resistance alleles are believed to offer selective advantages to the mosquitoes infected with *Plasmodium*; however, the fitness costs of these alleles have not been experimentally tested. To explore the impact of *TEP1* polymorphism on the fertility of irradiated males, we generated three *S1/S1*, *S2/S2*, and *R1/R1* homozygous lines from the *TEP1*-heterozygous *T4* line of *A. gambiae* obtained from Imperial College, London ([S6 Fig](#)). Indeed, *TEP1* genotyping of this line identified the following frequencies of *TEP1* alleles: *R1* (14%), *S1* (67%), and *S2* (19%). To obtain *TEP1* homozygous lines, the legs of virgin females and males were used for nested PCR-restriction fragment length polymorphism (RFLP) genotyping, and the reciprocal crosses were set up between the selected individuals. Once the *TEP1* homozygosity of the established lines was confirmed, male pupae from each line were irradiated, and the testes of the resulting males were dissected, stained, and microscopically examined. Lower numbers of TUNEL-positive cells were observed in the testes of *S2/S2* as compared to *S1/S1* and *R1/R1* males ([Fig 3B](#)). Moreover, the progeny of *S2/S2* males had higher hatching rates than *S1/S1* and *R1/R1* irradiated males ([Fig 3C](#)). Importantly, no differences were observed between these lines in the absence of radiation. These results suggest that the *TEP1*\**S2* allele efficiently protects against radiation-induced male sterility. To exclude the possibility that the observed differences were caused by variation at an unrelated locus, we generated heterozygous *S1*, *S2*, and *R1* males depleted for TEP1 by crossing *TEP1* homozygous

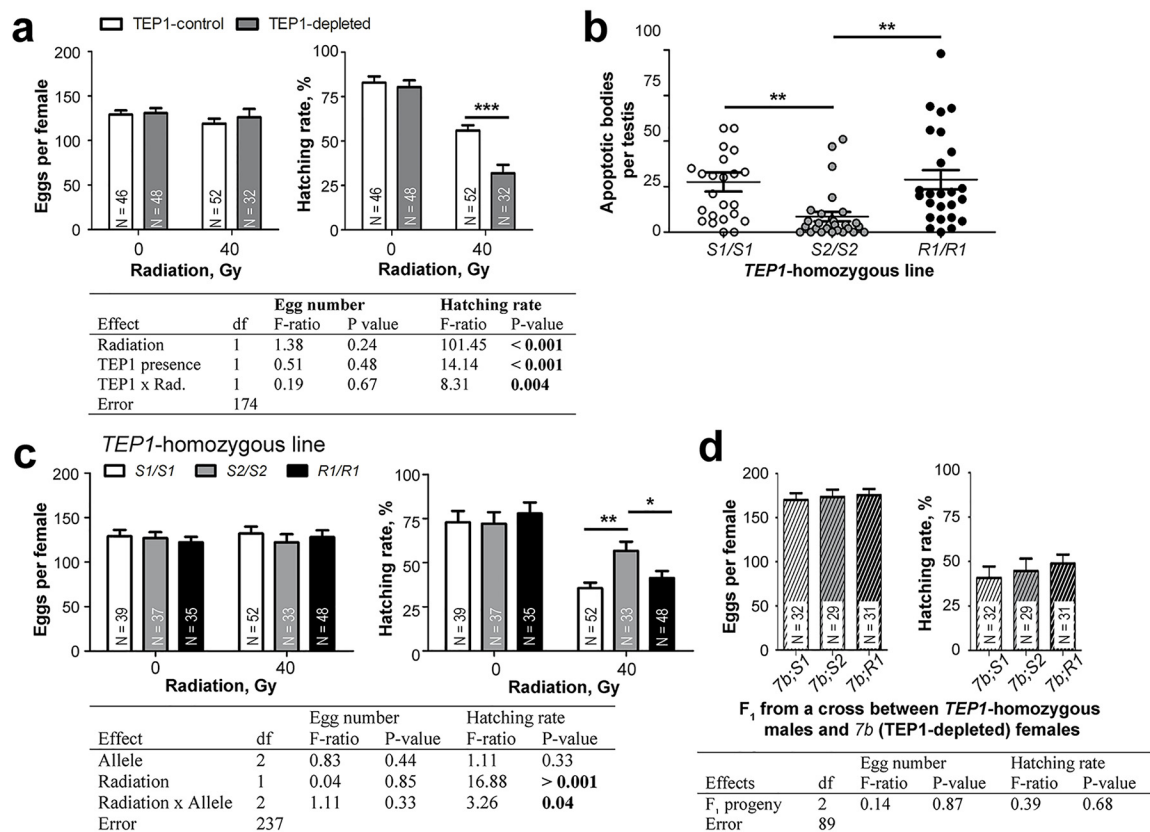


**Fig 3. Effect of radiation and TEP1 depletion on male fertility.** Pupae were irradiated (40 Gy), and the resulting 3-d-old males were mated with 3-d-old females. The mean  $\pm$  SEM of laid eggs and the proportions of hatched larvae are plotted. N, number of oviposited females. (A) After irradiation, TEP1 depletion (*7b* line) decreases hatching rates as compared to controls (*T4* line). (B) The proportion of testes with apoptotic cells was examined by TUNEL staining in irradiated *TEP1*-homozygous (*S1/S1*, *S2/S2*, or *R1/R1*) 1-d-old males. Each dot represents one testis. (C) Irradiated *TEP1*-homozygous (*S1/S1*, *S2/S2*, or *R1/R1*) 3-d-old males were mated with *TEP1*\**S1/S1* females. (D) *TEP1* expression was silenced in the males of F<sub>1</sub> reciprocal crosses between *7b* and each of the *TEP1*-homozygous lines. Irradiated F<sub>1</sub> 3-d-old males were mated with *TEP1*\**S1/S1*-homozygous females. The results of two-way analysis of variance (ANOVA) tests are shown in tables below the corresponding graphs. Post hoc Tukey's test: \*  $p < 0.05$ ; \*\*  $p < 0.01$ ; \*\*\*  $p < 0.001$ . Data used to make this figure can be found in [S1 Data](#).

doi:10.1371/journal.pbio.1002255.g003

males from each of the three lines with *7b* females (S6 Fig). Pupae of the resulting progeny were irradiated, and the obtained TEP1-depleted 3-d-old males were crossed with *TEP1*\**S1*-homozygous females. Similar sizes of egg batches and egg-hatching rates indicated that TEP1 depletion abrogated fertility advantages of the *S2* allele (Fig 3D). Taken together, our results indicate the allele-specific contribution of *TEP1* to higher male fertility rates in stressful conditions induced by radiation.

### Allele-Specific Role of *TEP1* in Male Fertility

We next evaluated whether TEP1 regulated male fertility under normal conditions. The radiation experiments described above were performed with young males (3-d-old). However, age plays a critical role in male mating behavior and insemination success. Although 3-d-old males are sexually competent, mosquito males show the highest levels of mating activity and form mating swarms several days later (7 to 9 d after emergence) [23,24]. Therefore, we compared the fertility of young (3-d-old) and mature (9-d-old) control and TEP1-depleted males.



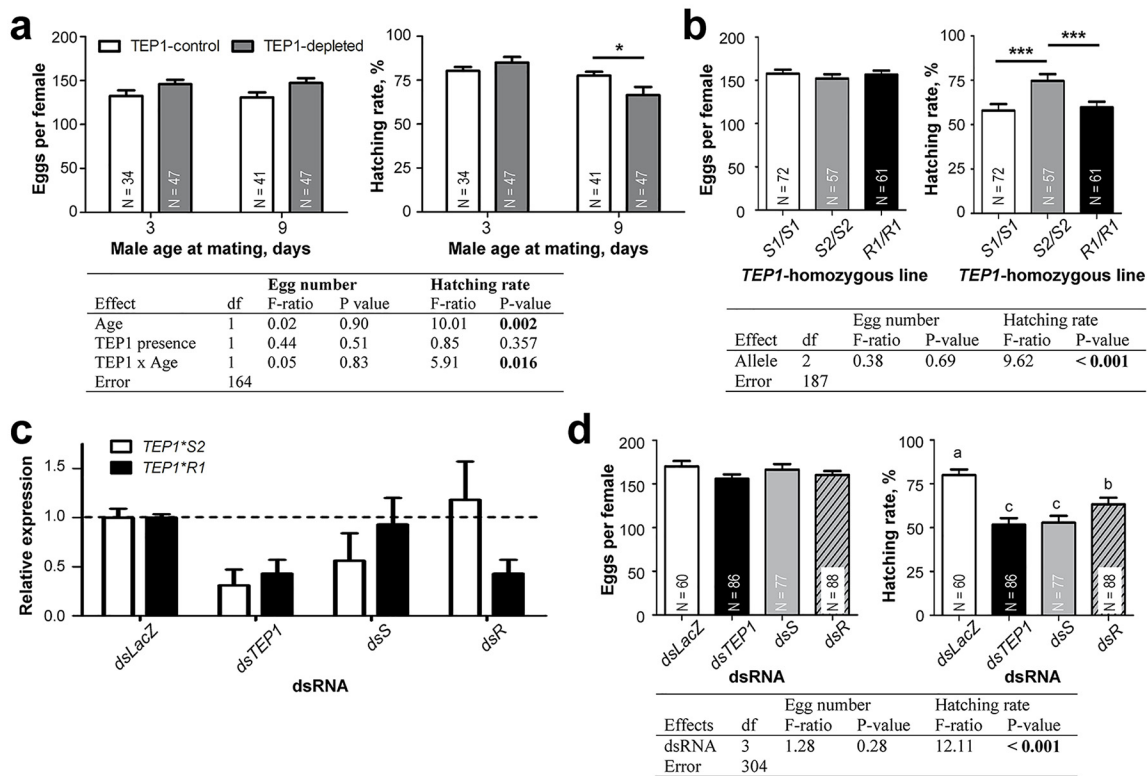


**Fig 4. Allele-specific function of TEP1 in male fertility.** Males (3- and 9-d-old) were mated with 3-d-old females. The mean  $\pm$  SEM of laid eggs and the proportions of hatched larvae are plotted. N, number of oviposited females. (A) Fertility rates of TEP1-depleted (7b line) and TEP1-control (7a line) males. (B) The fertility of TEP1-homozygous (S1/S1, S2/S2, or R1/R1) males mated with TEP1\*S1/S1 females. (C) 1-d-old TEP1\*S2/R1 males were injected with dsTEP1\*S2- (dsS) or with dsTEP1\*R1- (dsR), and 12 d later, relative expression levels of TEP1 were gauged by allele-specific quantitative reverse transcription PCR (qRT-PCR). Injection of dsLacZ and dsTEP1 served as a negative and a positive control, respectively. Expression of a gene encoding ribosomal protein L19 (*RpL19*) was used for normalization. Results of three independent experiments are plotted. (D) 1-d-old TEP1\*S2/R1 males were injected with dsTEP1\*S2- (dsS) or with dsTEP1\*R1- (dsR) and mated 8 d later with TEP1\*S1/S1 females. Injection of dsLacZ and dsTEP1 served as a negative and a positive control, respectively. Results of two-way ANOVA tests are shown in tables below the corresponding graphs. Statistically significant differences in (A,B): \*  $p < 0.05$ ; \*\*\*  $p < 0.001$ , post hoc Tukey's test, and in (D):  $p < 0.05$  (Fisher's LSD test), are indicated by characters above the corresponding values. Data used to make this figure can be found in [S1 Data](#).

doi:10.1371/journal.pbio.1002255.g004

Moderate but significantly lower hatching rates were observed in the progeny of mature but not young TEP1-depleted males as compared to same-age controls (Fig 4A), demonstrating that TEP1 regulates male fertility in the absence of radiation. To make sure that the observed phenotype was due to clearance of damaged sperm cells and not a consequence of microbial infections in TEP1-depleted mosquitoes, we examined bacterial loads in the testes and male accessory glands (MAGs) of control and TEP1-depleted 1- and 13-d-old mosquitoes by quantitative PCR of the conserved bacterial 16S rRNA gene. No significant differences between the two groups were detected (S7 Fig), indicating that TEP1 depletion did not cause significant changes in microbiota proliferation in male reproductive tissues that could explain the observed impact of TEP1 depletion on male sterility.

To validate the specific contribution of the TEP1\*S2 allele to male fertility, we compared the fertility rates of mature males of the TEP1 S1/S1, S2/S2, or R1/R1 homozygous lines described above. As in the radiation experiments, significantly higher hatching rates were detected in the progeny of S2/S2 males (Fig 4B). The causative effect of the TEP1 polymorphism was further validated by reciprocal allele-specific RNA interference, which interrogates the effects of allele-



specific silencing in an identical genetic background [21]. To this end, we performed reciprocal crosses between *R1/R1* and *S2/S2* homozygous lines and used males of  $F_1$  progeny heterozygous for *TEP1* (*S2/R1*) for injections with allele-specific dsRNAs targeting *S2* (*dsS*) or *R1* (*dsR*). Injections of *dsLacZ* and *dsTEP1* served as negative and positive controls, respectively. A significant reduction in the expression of targeted alleles was confirmed by quantitative PCR (Fig 4C). A moderate but significant decrease in hatching rates was detected in the progeny of *dsS*- and *dsTEP1*-depleted males (Fig 4D), thereby confirming the role of the *S2* allele in male fertility. We noted that the progeny of *dsR*-injected males displayed reduced hatching rates as compared to control *dsLacZ*, pointing towards epistatic interactions between *TEP1* alleles. Taken together, these data demonstrate the contribution of *TEP1*\**S2* allele to male fertility, thereby raising a possibility of a fitness trade-off between *TEP1* alleles in reproduction and immunity.

## Discussion

We discovered a new function of the complement-like cascade in spermatogenesis that impacts male fertility in the malaria mosquito. We demonstrate that depletion of the complement-like factor *TEP1* results in accumulation of defective sperm and decreases male fertility. Our study extends the role of the mosquito complement-like cascade from immunity to the removal of defective sperm during spermatogenesis and, thereby, to male fertility and reproduction.

We also show that *TEP1* function in spermatogenesis is regulated by the same HPX2-LRIM1 axis that controls killing of *Plasmodium* parasites in the midgut. We propose that activation of the *TEP1*/LRIM1/APL1C complex is induced by an unknown mechanism in the proximity of the damaged sperm cells. It appears that the surface modification mediated by HPX2 is required for *TEP1* binding to the damaged sperm, suggesting that the same signals are used by the mosquitoes to label defective cells and invading pathogens (S8 Fig). This conserved requirement for reactive nitrogen species in the activation of the mosquito complement-like system in immunity and reproduction suggests that nitration through oxidation of cell surface proteins may be a general mechanism of complement activation, which may be relevant for the activation of the alternative complement pathway in mammals (S8 Fig). The role of the complement factor C3, a mammalian homologue of *TEP1*, in the clearance of apoptotic bodies is well documented [17,25]. However, C3 deficient mice are fully fertile, and sperm quality is kept in check by a complement-independent mechanism, probably to prevent a deleterious complement activation on self surfaces and gamete damage [26]. Future studies should examine the mechanism(s) that mediate(s) removal of damaged cells and of invading parasites. In *Drosophila*, electron microscopy detected traces of the abnormal sperm in the neighboring cells but also inside the macrophage-like cells present in the testis tissues [27]. Although phagocytosis may contribute to the removal of the damaged sperm cells, this process is irrelevant for parasite clearance in the midgut, as no phagocytic cells have been detected by electron microscopy [28].

Previous reports demonstrated the causative role of the *R1* allele in mosquito resistance to infections with *Plasmodium berghei* and with some isolates of *P. falciparum* [21,22,29,30]. However, low rates of infected mosquitoes in natural populations question the impact of *Plasmodium* on *TEP1* evolution. Given the broad function of *TEP1* in immune responses to bacteria and fungi [19,31–33], local microbial pressures on the larval stages may drive its exceptional variability across Africa [22], a hypothesis that has never been experimentally proven. Here we show that *TEP1* affects reproduction at the age when males actively engage in mating, suggesting that our findings are relevant for male fitness in natural mosquito populations. Moreover, we report that in contrast to resistance to *Plasmodium*, a distinct “susceptible” *S2* allele mediates higher male fertility rates. At the structural level, the *S2* form of *TEP1* is

mostly similar to the S1 form, except for a  $\beta$ -hairpin loop, shared with R1 and R2 and located on the convex surface of the thioester domain [34]. The exposed position of this loop is suggestive of its role in protein–protein interactions. Although interactions with distinct partners may define a critical role of S2 form in cell removal, further studies are needed to examine biochemical bases of *TEP1* pleiotropism. A recent report demonstrated the role of the mosquito heme peroxidase 15 (HPX15) in long-term female fertility by protecting sperm from oxidative damage during storage in spermathecae [35]. The results presented here uncover the role of the HPX2/*TEP1*/LRIM1 complement-like cascade in the removal of defective sperm cells in the testes, the process that promotes male fertility rates. As strong selective pressures apply to genes involved in reproduction [36] and male fitness [37], even the moderate contribution of S2 to male fertility revealed in our experiments may have important consequences for mosquito field populations, as enrichment in S2 alleles may render mosquito populations more susceptible to *Plasmodium* infections. Taken together, we propose that pleiotropic antagonism may drive the evolution of the *TEP1* locus and shape the genetic makeup of resistance to *Plasmodium* in a major malaria vector.

## Methods

### Ethics Statement

All work in this study was performed in agreement with national animal work authorization E 67-484-2 issued by the Department of Veterinary Services, Prefecture du Bas-Rhin, France.

### Mosquito Strains

*A. gambiae* sensu stricto strain G3 and *TEP1* homozygous and transgenic lines originating from it were used throughout the study. Mosquitoes were reared in the insectary at  $28 \pm 2^\circ\text{C}$  and  $80 \pm 5\%$  humidity with a 12/12 h dark/light cycle. Larvae were fed with grinded fish food (Tetra), and adults received a 10% sugar solution (w/v). All work in this study was performed in agreement with national animal work authorization E 67-482-2 issued by the Department of Veterinary Services, Prefecture du Bas-Rhin, France.

**Transgenic lines.** The *DSX* line (*TEP1*\**S1/S1*) expressed three reporters: (i) a *3xP3::DsRed* transgenesis marker in the mosquito nervous system [38]; (ii) a  *$\beta$ -tubulin::eGFP* reporter expressed in spermatocytes, spermatids, and spermatozoa; and (iii) a *DmActin5C::eGFP* reporter expressed predominantly in the midgut [12]. *DSX* mosquitoes were used to differentiate spermatogenic compartments in the testes.

The *7b* line (*TEP1*\**S1/S1*) was obtained by a piggyBac-mediated transgene insertion on the X chromosome. The transgene contains (i) a *3xP3::DsRed* transgenesis marker expressed in the mosquito nervous system [38] and (ii) a *DmHsp70::TEP1* cassette that causes a dominant depletion of *TEP1* (S2 Fig). *7b* mosquitoes were used as a positive control for experiments testing the effect of *TEP1* depletion on spermatogenesis and on male fertility, while the transgenesis *3xP3::DsRed* marker of this line inserted on the X chromosome was used to sex larvae at an early stage, using a COPAS instrument (Union Biometrica) as described [39] to ensure adults' virginity.

The *T4* line, obtained from the Imperial College, London, expressed the *3xP3::eGFP* reporter in the nervous system of males but not females because of the piggyBac transposon insertion on the Y chromosome [40]. This line was used for high-throughput male selection using the COPAS instrument. Genotyping of the *T4* line showed that it was heterozygous for *TEP1* and contained *R1* (14%), *S1* (67%), and *S2* (19%) alleles; therefore, we used this line for establishment of the *TEP1* homozygous lines.

***TEP1* homozygous lines.** To establish *TEP1*-homozygous lines from the heterozygous *T4* population, legs from 192 live males and 192 live females were genotyped by the PCR-RFLP method described below. Individuals (25 males and 25 females) with the selected genotypes for each homozygous line were used for crosses. After three rounds of intracrossing, the resulting *TEP1*\**S1/S1*, *S2/S2*, and *R1/R1* lines were established and used for experiments within the next five generations.

## Genetic Crosses

F<sub>1</sub> progenies of the reciprocal crosses between *DSX* and *7b* lines were used for experiments with *7b*; *DSX* and wt; *DSX* males. To obtain *7b/S1*, *7b/S2*, and *7b/R1* heterozygous males, F<sub>1</sub> progenies of crosses between *7b* females and *TEP1*\**S1/S1*, \**S2/S2*, and \**R1/R1* homozygous males were used. Males heterozygous for *TEP1*\**S2/R1* were from the F<sub>1</sub> progeny of a cross between *TEP1*\**R1/R1* females and *TEP1*\**S2/S2* males. The COPAS instrument (Union Biometrica) was used for sexing of the early larval stages [39]. Females and males of *DSX*, *TEP1*-homozygous, and *7b* lines were raised separately, and 100 males and 50 females were mated in each cross.

## *TEP1* Genotyping

To identify *TEP1* alleles in the mosquito lines used in this study, we used a nested PCR-RFLP. DNA was extracted from one mosquito leg in 40  $\mu$ l of grinding buffer (10 mM Tris-HCl pH 8.2; 1 mM EDTA; 25 mM NaCl) mixed with 0.4  $\mu$ l of 100x Proteinase K (Sigma) and incubated for 45 min at 37°C. A first PCR was conducted using VB3 5'-ATGTGGTGAGCAGAATATGG-3' and VB4 5'-ACATCAATTTGCTCCGAGTT-3' primers, followed by a second PCR performed on 2  $\mu$ l of the resulting product with AG1656 5'-ATCTAATCGACAAAGCTACGAA TTT-3' and AG1653 5'-CTTCAGTTGAACGGTGTAGTCGTT-3' primers, producing a final fragment of 764 bp. Both PCR reactions were subjected to 95°C for 2 min, 30 cycles with 15 s at 95°C, 15 s at 55°C, and 45 s at 72°C, and a final step at 72°C for 5 min, using GO Tag Green Master mix (Promega). PCR products were digested by *Bam* HI, *Hind* III, or *Bse* NI (Fermentas) and analyzed on 1.5% agarose gels. Expected restriction patterns are provided in [S1 Table](#). Genotyping was conducted on 96 males and 96 females from *T4*, *DSX*, *7b*, and on each of the *TEP1*-homozygous and *TEP1*-heterozygous lines.

## *TEP1* Sequencing

Verification of *TEP1* sequences from homozygous lines was obtained by amplicon sequencing as described [21] using DNA extracts of five different mosquitoes for each line. DNA was extracted using the DNeasy kit (QIAGEN). Sequencing revealed that *TEP1*\**S1* corresponded to the *TEP1*\**S4* allele initially identified in the *VKper* line, *TEP1*\**S2* to the *TEP1*\**S6* allele from the Nguosso, and *TEP1*\**R1* to the *TEP1*\**R1* from the L3-5 refractory line [21,29].

## Immunofluorescence and Confocal Microscopy

To examine the presence of *TEP1*, *HPX2*, and *LRIM1*, the testes were dissected in 1x PBS, fixed with 2% PFA in 1x PBS for 1 h; permeabilized with 0.5% Triton in 1x PBS for 20 min; blocked with 0.5% Triton, 1% BSA, in 1x PBS for 30 min; incubated overnight at 4°C with anti-*TEP1* (1/300) [41], the anti-*HPX2* [7], or anti-*LRIM1* [5] polyclonal rabbit antibodies in the blocking solution and then washed with 0.5% Triton, 1% BSA, in 1x PBS; and incubated for 2 h with a secondary fluorescence-labeled Cy3 or Cy5 anti-rabbit IgG antibody (1/1,000) (Jackson Laboratory) and DAPI (1/5,000) (Vector Laboratories) in the blocking solution for 15 min.

To reveal DNA damage, the TUNEL assay was performed on TEP1-stained testes dehydrated for 3 h on SuperFrost/Plus slides (Menzel-Glazer) using the ApopTag Red *In Situ* kit (Millipore).

To determine TEP1 occurrence in the testes after mating, 2-d-old virgin males were added to a cage containing virgin females, and couples were collected *in copula* within the first hour. Males were then kept in a separate cage for 2 d. The testes were dissected and assessed for TEP1 presence using anti-TEP1 polyclonal antibodies and immunofluorescence.

All samples were mounted in Vectashield medium (Vector Laboratories), examined using a LSM700 laser confocal microscope (Zeiss), and analyzed using Image J open source software [42] with the Figure J package [43].

## Immunoblotting

To determine the presence of TEP1, LRIM1, or HPX2 in the hemolymph or the testes, hemolymph samples from ten mosquitoes were collected by proboscis clipping, and the testes extracts were obtained by grinding 20 dissected testes in 10  $\mu$ l of Laemmli buffer (Tris-HCl 0.35 M; 10.3% SDS; 36% glycerol; 5%  $\beta$ -mercaptoethanol; 0.012% bromophenol blue). Extracts were separated by precast 4%–20% gradient SDS-PAGE (Bio-Rad). Protein membrane transfer, antibody incubations, and detection were carried out, as previously described [41], using anti-TEP1 [41] (1/1,000) and anti-LRIM1 [5] antibodies (1/300), with anti-prophenoloxidase 2 (PPO2) (1/15,000) or anti- $\alpha$ -actin antibody (1/1,000) (Chemicon) as loading controls. Immunoblotting of HPX2 was conducted in native conditions as described [7]. Bound antibodies were detected by an anti-rabbit or anti-mouse IgG conjugated to horseradish peroxidase (1/30,000) (Promega) using Super Signal West Pico Chemiluminescent Substrate (Thermo Scientific).

## RNAi Silencing

To deplete TEP1, LRIM1, TEP1\*S, or TEP1\*R, dsRNAs for *TEP1*, *LRIM1*, *LacZ*, *TEP1\*S* (*dsS*), and *TEP1\*R* (*dsR*) were produced from plasmids containing the dsRNA-target sequence flanked by two *T7* promoters [5,21,44]. To deplete HPX2, dsRNA for *HPX2* was produced from PCR-amplified fragments flanked with two *T7* promoters as described [7]. RNA synthesis and purification were performed using MegaScript and MegaClear kits (Ambion). RNA concentrations were measured by Nanodrop (Thermo Scientific) before annealing 3  $\mu$ g/ $\mu$ l of sense and anti-sense RNAs by boiling. DsRNAs were injected (69 nl) into the thorax of CO<sub>2</sub>-immobilized 1-d-old mosquitoes using a glass capillary mounted onto a Nanoject II injector (Drummond).

## Quantitative Reverse Transcription PCR

To quantify the mRNA level for *TEP1*, *LRIM1*, and *HPX2*, total RNA was extracted from ten mosquitoes using the RNeasy extraction kit (QIAGEN) or RNazol (Sigma-Aldrich) and reverse-transcribed by the M-MuLV Reverse Transcription kit (Thermo Scientific). Gene expression was quantified using primers and probes detailed in S2 Table by quantitative PCR with Fast SybrGreen chemistry for *LRIM1* and *HPX2* and TaqMan chemistry for *TEP1* and *RPL19*, using the ABI 7500 Fast Real-Time PCR machine. Expression of *RPL19*, the gene encoding housekeeping ribosomal protein L19, was used for normalization.



## $\gamma$ -Ray Irradiation

To induce sperm damage, pupae were subjected to radiation within the first 12 h after pupation using a Biobeam 8000 (Gamma-Service Medical Research).

## Fertility Assays

To estimate the impact of TEPI presence or the *TEPI* allele on male fertility, female and male larvae were sexed by the COPAS instrument and raised separately [39]. On day 3 after emergence, 25 virgin females were mixed with 50 virgin males in a cubic 17 cm cage. Females were fed on a mouse 5 d later, and unfed females were removed from the cage. On day 7, individual females were placed into plastic vials containing 1–2 ml of water and closed with cotton pads. On days 9–10, the deposited eggs and larvae were counted in each vial. We confirmed that females that did not lay eggs had no sperm in their spermathecae, as previously reported [45]. For fertility assays with mature males, males were kept virgin, and on day 9 after emergence, they were mated to 3-d-old females and assessed as above. Experiments were repeated four times: two independent experiments with two different cages.

## Estimation of Bacterial Loads

To examine the effect of TEPI depletion on bacterial loads in the male sexual organs, control (*T4*) and TEPI-depleted (*7b*) larvae were reared in the same water to ensure equal exposure to the environmental microbes. The adults were separated after eclosion based on expression of fluorescent markers. On days 1 and 13 after emergence, the testes and MAGs were dissected from five adults per group, and DNA was extracted using the DNeasy kit (QIAGEN). Bacterial loads were gauged by quantitative PCR of the highly conserved *16S* rRNA gene (S2 Table) [46]. Three independent biological experiments were conducted.

## Statistical Analysis

Normalization of the distribution and the homogeneity of variances was evaluated by Shapiro's and Bartlett's tests, respectively. To fit normal distribution and homogeneity of variances, larval hatching rates were arcsin square root-transformed before analysis. Statistical analyses were conducted using SYSTAT 12.0 (SYSTAT software) and R (<http://www.R-project.org>) software.

## Supporting Information

**S1 Data. Raw data used to generate plots in Figs 1F, 1G, 2A–2C, 2H, 2I, 3A–3D, and 4A–4D and S7 Fig.**

(XLSX)

**S1 Fig. A high level of radiation (100 Gy) destroys spermatogonial compartment of the testes of 3-d-old males.** *DSX* [12] pupae were irradiated and observed with confocal microscopy 3 d after adult emergence.

(TIF)

**S2 Fig. TEPI is absent from the testes of *7b* and *dsTEPI*-injected males.** (A) TEPI protein levels in the testes of 3- and 14-d-old *7b* and *T4* males that were either not injected or injected with *dsLacZ* or with *dsTEPI* on day 1 after emergence. Testes' protein extracts were immunoblotted with anti-TEPI antibodies and anti- $\alpha$ -actin antibody as a protein loading control. (B, C) One-d-old *DSX* males were injected with dsRNA. Two d later, the testes were dissected, stained for TEPI by immunofluorescence analysis using anti-TEPI polyclonal antibodies, and observed using confocal microscopy. TEPI was detected in the testes of *dsLacZ*-injected males

(B–B') but not in *dsTEP1*-injected males (C–C'). (D) Testes from 3-d-old *7b* (TEP1-depleted) males were dissected, stained for TEP1 by immunofluorescence analysis using anti-TEP1 polyclonal antibodies, and observed using confocal microscopy. TEP1 signal was not detected in the testes of *7b* males.

(TIF)

**S3 Fig. The presence of HPX2 and LRIM1 in the testes.** (A) HPX2 (red) and (B) LRIM1 (red) are detected in the cells surrounding the testes. Nuclei are colored by DAPI (blue). *T4* males were dissected, stained with antibody against HPX2 or LRIM1, and observed using confocal microscopy.

(TIF)

**S4 Fig. DsRNA injection efficiently depletes LRIM1, HPX2, and TEP1 in mosquitoes.** One-day-old males were injected with dsRNA, and 2 d later, their hemolymph was extracted for immunoblotting analyses. Injection of *dsLacZ* was used as a negative control. A hemolymph-borne enzyme, prophenoloxidase 2 (PPO2), served as a protein loading control. (A) Silencing of *LRIM1* reduces LRIM1 protein level, while silencing of *LRIM1* and *HPX2* does not affect protein levels of full-length TEP1 (TEP1-F). Note that in the absence of LRIM1, TEP1-cut is no longer detected. (B) Silencing of *HPX2* significantly reduces HPX2 protein levels.

(TIF)

**S5 Fig. TEP1 is depleted from the hemolymph of control and irradiated (40 Gy) *7b*; *DSX* heterozygous males.** Hemolymph of F<sub>1</sub> males from the reciprocal crosses between *DSX* and *7b* was extracted on the day of emergence for immunoblotting analyses using anti-TEP1 antibodies. A hemolymph-borne enzyme, PPO2, served as a protein loading control.

(TIF)

**S6 Fig. TEP1 protein levels in the hemolymph are identical among the three *TEP1*-homozygous lines and depleted in the F<sub>1</sub> progeny of reciprocal crosses between *7b* and the *TEP1*-homozygous lines.** Hemolymph was extracted from male mosquitoes on the day of emergence for immunoblotting analyses. A hemolymph-borne enzyme, PPO2, served as a protein loading control.

(TIF)

**S7 Fig. TEP1 depletion does not affect bacterial loads in male sexual organs.** Bacterial loads were gauged in the testes and MAGs of control (*T4*) and TEP1-depleted (*7b*) 1- and 13-d-old males by quantitative PCR of the conserved bacterial 16S rRNA gene. Larvae of control and TEP1-depleted mosquitoes were raised in the same water and separated at the adult stage according to the expression of fluorescence markers. Three biological repetitions were conducted, each represented by a dot. Fold-change differences in bacterial loads between control and TEP1-depleted mosquitoes are shown. Statistical analysis was performed by two-way ANOVA tests summarized in the tables below the graph. Data used to make this figure can be found in [S1 Data](#).

(TIF)

**S8 Fig. Comparison of the mosquito complement-like and the mammalian alternative complement activation pathways.** Unlike the classical or lectin pathways, in which complement activation is directed to self and nonself surfaces modified by antibody or lectin, respectively, the activation of the alternative pathway is thought to result from a constant spontaneous activation of C3, amplified at the surfaces by the C3b convertase [47]. Conserved requirement for reactive nitrogen species (RNS) in the activation of the mosquito complement-like system revealed here led us to speculate that nitration may play an equally important role in targeting

the complement activation to self and nonself in mammals. The mosquito complement-like pathway was designed following the previous studies [5–7,41,48,49].

(TIF)

**S1 Table. TEP1 genotyping by nested PCR and RFLP.**

(DOCX)

**S2 Table. Primers and probes used for qRT-PCR.**

(DOCX)

## Acknowledgments

The authors are grateful to Dr. C. Barillas-Mury for the HPX2 antibody, Prof. F. Catteruccia for the *DSX* line, and Dr. N. Windbichler for the *T4* line and thank J. Soichot, N. Schallon, and Dr. N. Jelly for help with mosquito colonies. We thank our colleagues and lab members for fruitful discussions and Dr. R. Willmott (BioScript International) for editorial assistance. JP was a fellow of the Fondation pour la Recherche Médicale and the Fondation les Treilles.

## Author Contributions

Conceived and designed the experiments: JP EAL. Performed the experiments: JP. Analyzed the data: JP EAL. Contributed reagents/materials/analysis tools: JP EAL. Wrote the paper: JP EAL.

## References

1. Blandin S, Levashina EA. Thioester-containing proteins and insect immunity. *Mol Immunol*. 2004; 40(12):903–8. PMID: [14698229](#)
2. Dong YM, Aguilar R, Xi ZY, Warr E, Mongin E, Dimopoulos G. *Anopheles gambiae* immune responses to human and rodent *Plasmodium* parasite species. *PLoS Pathog*. 2006; 2(6):513–25.
3. Molina-Cruz A, Garver LS, Alabaster A, Bangiolo L, Haile A, Winikor J, et al. The Human malaria parasite *Pfs47* gene mediates evasion of the mosquito immune system. *Science*. 2013; 340(6135):984–7. doi: [10.1126/science.1235264](#) PMID: [23661646](#)
4. Nsango SE, Abate L, Thoma M, Pompon J, Fraiture M, Rademacher A, et al. Genetic clonality of *Plasmodium falciparum* affects the outcome of infection in *Anopheles gambiae*. *Int J Parasitol*. 2012; 42(6):589–95. doi: [10.1016/j.ijpara.2012.03.008](#) PMID: [22554991](#)
5. Fraiture M, Baxter RHG, Steinert S, Chelliah Y, Frolet C, Quispe-Tintaya W, et al. Two mosquito LRR proteins function as complement control factors in the TEP1-mediated killing of *Plasmodium*. *Cell Host & Microbe*. 2009; 5(3):273–84.
6. Povelones M, Waterhouse RM, Kafatos FC, Christophides GK. Leucine-rich repeat protein complex activates mosquito complement in defense against *Plasmodium* parasites. *Science*. 2009; 324(5924):258–61. doi: [10.1126/science.1171400](#) PMID: [19264986](#)
7. Oliveira GdA, Lieberman J, Barillas-Mury C. Epithelial nitration by a peroxidase/NOX5 system mediates mosquito antiplasmodial immunity. *Science*. 2012; 335(6070):856–9. doi: [10.1126/science.1209678](#) PMID: [22282475](#)
8. Osta MA, Christophides GK, Kafatos FC. Effects of mosquito genes on *Plasmodium* development. *Science*. 2004; 303(5666):2030–2. PMID: [15044804](#)
9. Riehle MM, Markianos K, Niare O, Xu J, Li J, Toure AM, et al. Natural malaria infection in *Anopheles gambiae* is regulated by a single genomic control region. *Science*. 2006; 312(5773):577–9. PMID: [16645095](#)
10. Clements AN. Spermatogenesis and the structure of spermatozoa. London: Chapman & Hall; 1992. 333–9 p.
11. Catteruccia F, Benton JP, Crisanti A. An *Anopheles* transgenic sexing strain for vector control. *Nat Biotechnol*. 2005; 23(11):1414–7. PMID: [16244659](#)
12. Magnusson K, Mendes AM, Windbichler N, Papathanos P-A, Nolan T, Dottorini T, et al. Transcription regulation of sex-biased genes during ontogeny in the Malaria vector *Anopheles gambiae*. *PLoS ONE*. 2011; 6(6).

13. Mahmood F, Reisen WK. *Anopheles stephensi* (Diptera: Culicidae): changes in male mating competence and reproduction system morphology associated with aging and mating. *J Med Entomol*. 1982; 19(5):573–88. PMID: [7143380](#)
14. Abrams JM, White K, Fessler LI, Steller H. Programmed cell death during *Drosophila* embryogenesis. *Development*. 1993; 117(1):29–43. PMID: [8223253](#)
15. Blanco R. A matter of death and life: the significance of germ cell death during spermatogenesis. *Int J Androl*. 1998; 21(5):236–48. doi: [10.1046/j.1365-2605.1998.00133.x](#) PMID: [9805237](#)
16. Helinski MEH, Parker AG, Knols BGJ. Radiation-induced sterility for pupal and adult stages of the malaria mosquito *Anopheles arabiensis*. *Malaria Journal*. 2006; 5(41):1–10.
17. Fishelson Z, Attali G, Mevorach D. Complement and apoptosis. *Mol Immunol*. 2001; 38(2–3):207–19. PMID: [11532282](#)
18. Lauber K, Blumenthal SG, Waibel M, Wesselborg S. Clearance of apoptotic cells: Getting rid of the corpses. *Mol Cell*. 2004; 14(3):277–87. PMID: [15125832](#)
19. Blandin S, Shiao S-H, Moita LF, Janse CJ, Waters AP, Kafatos FC, et al. Complement-like protein TEP1 is a determinant of vectorial capacity in the malaria vector *Anopheles gambiae*. *Cell*. 2004; 116(5):661–70. PMID: [15006349](#)
20. Obbard D, Callister D, Jiggins F, Soares D, Yan G, Little T. The evolution of *TEP1*, an exceptionally polymorphic immunity gene in *Anopheles gambiae*. *BMC Evol Biol*. 2008; 8(1):274.
21. Blandin SA, Wang-Sattler R, Lamacchia M, Gagneur J, Lycett G, Ning Y, et al. Dissecting the genetic basis of resistance to malaria parasites in *Anopheles gambiae*. *Science*. 2009; 326(5949):147–50. doi: [10.1126/science.1175241](#) PMID: [19797663](#)
22. White BJ, Lawniczak MKN, Cheng CD, Coulibaly MB, Wilson MD, Sagnon N, et al. Adaptive divergence between incipient species of *Anopheles gambiae* increases resistance to *Plasmodium*. *Proc Natl Acad Sci U S A*. 2011; 108(1):244–9. doi: [10.1073/pnas.1013648108](#) PMID: [21173248](#)
23. Verhoek BA, Takken W. Age effects on the insemination rate of *Anopheles gambiae* sl in the laboratory. *Entomol Exp Appl*. 1994; 72(2):167–72.
24. Sawadogo SP, Diabate A, Toe HK, Sanon A, Lefevre T, Baldet T, et al. Effects of age and size on *Anopheles gambiae* s.s. male mosquito mating success. *J Med Entomol*. 2013; 50(2):285–93. PMID: [23540115](#)
25. Trouw LA, Blom AM, Gasque P. Role of complement and complement regulators in the removal of apoptotic cells. *Mol Immunol*. 2008; 45(5):199–207. PMID: [17961651](#)
26. Qin XB, Dobarro M, Bedford SJ, Ferris S, Miranda PV, Song WP, et al. Further characterization of reproductive abnormalities in mCd59b knockout mice: A potential new function of mCd59 in male reproduction. *J Immunol*. 2005; 175(10):6294–302. PMID: [16272280](#)
27. Yacobi-Sharon K, Namdar Y, Arama E. Alternative germ cell death pathway in *Drosophila* involves HtrA2/Omi, lysosomes, and a Caspase-9 counterpart. *Dev Cell*. 2013; 25(1):29–42. doi: [10.1016/j.devcel.2013.02.002](#) PMID: [23523076](#)
28. Shiao S-H, Whitten MMA, Zachary D, Hoffmann JA, Levashina EA. Fz2 and Cdc42 mediate melanization and actin polymerization but are dispensable for *Plasmodium* killing in the mosquito midgut. *PLoS Pathog*. 2006; 2(12):e133. PMID: [17196037](#)
29. Collins F, Sakai R, Vernick K, Paskewitz S, Seeley D, Miller L, et al. Genetic selection of a *Plasmodium*-refractory strain of the malaria vector *Anopheles gambiae*. *Science*. 1986; 234(4776):607–10. PMID: [3532325](#)
30. Molina-Cruz A, DeJong RJ, Ortega C, Haile A, Abban E, Rodrigues J, et al. Some strains of *Plasmodium falciparum*, a human malaria parasite, evade the complement-like system of *Anopheles gambiae* mosquitoes. *Proc Natl Acad Sci U S A*. 2012; 109(28):1957–62.
31. Baxter RHG, Chang C-I, Chelliah Y, Blandin S, Levashina EA, Deisenhofer J. Structural basis for conserved complement factor-like function in the antimalarial protein TEP1. *Proc Natl Acad Sci U S A*. 2007; 104(28):11615–20. PMID: [17606907](#)
32. Moita LF, Wang-Sattler R, Michel K, Zimmermann T, Blandin S, Levashina EA, et al. *In vivo* identification of novel regulators and conserved pathways of phagocytosis in *A. gambiae*. *Immunity*. 2005; 23(1):65–73. PMID: [16039580](#)
33. Yassine H, Kamareddine L, Osta MA. The mosquito melanization response is implicated in defense against the entomopathogenic fungus *Beauveria bassiana*. *PLoS Pathog*. 2012; 8(11).
34. Le BV, Williams M, Logarajah S, Baxter RHG. Molecular basis for genetic resistance of *Anopheles gambiae* to *Plasmodium*: Structural analysis of TEP1 susceptible and resistant alleles. *PLoS Pathog*. 2012; 8(10):e1002958. doi: [10.1371/journal.ppat.1002958](#) PMID: [23055931](#)



35. Shaw WR, Teodori E, Mitchell SN, Baldini F, Gabrieli P, Rogers DW, et al. Mating activates the heme peroxidase HPX15 in the sperm storage organ to ensure fertility in *Anopheles gambiae*. *Proc Natl Acad Sci U S A*. 2014; 111(16):5854–9. doi: [10.1073/pnas.1401715111](https://doi.org/10.1073/pnas.1401715111) PMID: [24711401](https://pubmed.ncbi.nlm.nih.gov/24711401/)
36. Haerty W, Jagadeeshan S, Kulathinal RJ, Wong A, Ravi Ram K, Sirot LK, et al. Evolution in the fast lane: Rapidly evolving sex-related genes in *Drosophila*. *Genetics*. 2007; 177(3):1321–35. PMID: [18039869](https://pubmed.ncbi.nlm.nih.gov/18039869/)
37. Singh RS, Kulathinal RJ. Male sex drive and the masculinization of the genome. *BioEssays*. 2005; 27(5):518–25. PMID: [15832384](https://pubmed.ncbi.nlm.nih.gov/15832384/)
38. Horn C, Jaunich B, Wimmer EA. Highly sensitive, fluorescent transformation marker for *Drosophila* transgenesis. *Dev Genes Evol*. 2000; 210(12):623–9. PMID: [11151299](https://pubmed.ncbi.nlm.nih.gov/11151299/)
39. Marois E, Scali C, Soichot J, Kappler C, Levashina E, Catteruccia F. High-throughput sorting of mosquito larvae for laboratory studies and for future vector control interventions. *Malaria Journal*. 2012; 11(1):302.
40. Bernardini F, Galizi R, Menichelli M, Papathanos P-A, Dritsou V, Marois E, et al. Site-specific genetic engineering of the *Anopheles gambiae* Y chromosome. *Proc Natl Acad Sci U S A*. 2014; 111(21):7600–5. doi: [10.1073/pnas.1404996111](https://doi.org/10.1073/pnas.1404996111) PMID: [24821795](https://pubmed.ncbi.nlm.nih.gov/24821795/)
41. Levashina EA, Moita LF, Blandin S, Vriend G, Lagueux M, Kafatos FC. Conserved role of a complement-like protein in phagocytosis revealed by dsRNA knockout in cultured cells of the mosquito, *Anopheles gambiae*. *Cell*. 2001; 104(5):709–18. PMID: [11257225](https://pubmed.ncbi.nlm.nih.gov/11257225/)
42. Schneider CA, Rasband WS, Eliceiri KW. NIH Image to ImageJ: 25 years of image analysis. *Nat Meth*. 2012; 9:671–5.
43. Mutterer J, Zinck E. FigureJ. ImageJ Users and Developers Conference2012.
44. Blandin S, Moita LF, Köcher T, Wilm M, Kafatos FC, Levashina EA. Reverse genetics in the mosquito *Anopheles gambiae*: targeted disruption of the *Defensin* gene. *EMBO J*. 2002; 3(9):852–6.
45. Thailayil J, Magnusson K, Godfray HCJ, Crisanti A, Catteruccia F. Spermless males elicit large-scale female responses to mating in the malaria mosquito *Anopheles gambiae*. *Proc Natl Acad Sci U S A*. 2011; 108(33):13677–81. doi: [10.1073/pnas.1104738108](https://doi.org/10.1073/pnas.1104738108) PMID: [21825136](https://pubmed.ncbi.nlm.nih.gov/21825136/)
46. Nadkarni MA, Martin FE, Jacques NA, Hunter N. Determination of bacterial load by real-time PCR using a broad-range (universal) probe and primers set. *Microbiology*. 2002; 148(1):257–66.
47. Lambris JD, Reid KBM, Volanakis JE. The evolution, structure, biology and pathophysiology of complement. *Immunology Today*. 1999; 20(5):207–11. PMID: [10322298](https://pubmed.ncbi.nlm.nih.gov/10322298/)
48. Baxter RHG, Steinert S, Chelliah Y, Volohonsky G, Levashina EA, Deisenhofer J. A heterodimeric complex of the LRR proteins LRIM1 and APL1C regulates complement-like immunity in *Anopheles gambiae*. *Proc Natl Acad Sci U S A*. 2010; 107(39):16817–22. doi: [10.1073/pnas.1010575107](https://doi.org/10.1073/pnas.1010575107) PMID: [20826443](https://pubmed.ncbi.nlm.nih.gov/20826443/)
49. Povelones M, Bhagavatula L, Yassine H, Tan LA, Upton LM, Osta MA, et al. The CLIP-domain serine protease homolog SPCLIP1 regulates complement recruitment to microbial surfaces in the malaria mosquito *Anopheles gambiae*. *PLoS Pathog*. 2013; 9(9).